The Redox Chemistry of 4-Benzoyl-*N*-methylpyridinium Cations in Acetonitrile with and without Proton Donors: The Role of Hydrogen Bonding

Nicholas Leventis,*,† Ian A. Elder, Xuerong Gao, Eric W. Bohannan, Chariklia Sotiriou-Leventis,*,‡ Abdel Monem M. Rawashdeh, Travis J. Overschmidt, and Kimberly R. Gaston

Department of Chemistry, The University of Missouri at Rolla, 142 Schrenk Hall, Rolla, Missouri 65409-0010

Received: February 26, 2001

In anhydrous CH_3CN, 4-benzoyl-*N*-methylpyridinium cations undergo two reversible, well-separated ($\Delta E_{1/2} \sim 0.6$ V) one-electron reductions in analogy to quinones and viologens. If the solvent contains weak protic acids, such as water or alcohols, the first cyclic voltammetric wave remains unaffected while the second wave is shifted closer to the first. Both voltammetric and spectroelectrochemical evidence suggest that the positive shift of the second wave is due to hydrogen bonding between the two-electron reduced form of the ketone and the proton donors. While the one-electron reduction product is stable both in the presence and in the absence of the weak-acid proton donors, the two-electron reduction wave is reversible only in the time scale of cyclic voltammetry. Interestingly, at longer times, the hydrogen bonded adduct reacts further giving *nonquaternized* 4-benzoylpyridine and 4-(α-hydroxybenzyl)pyridine as the two main terminal products. In the presence of stronger acids, such as acetic acid, the second wave merges quickly with the first, producing an irreversible two-electron reduction wave. The only terminal product in this case is the *quaternized* 4-(α-hydroxybenzyl)-*N*-methylpyridinium cation. Experimental evidence points toward a common mechanism for the formation of the nonquaternized products in the presence of weaker acids and the quaternized product in the presence of CH_3CO_2H.

1. Introduction

In general, chemical or electrochemical reduction of ketones yields alcohols.[1] More specifically, in aprotic media electrochemical reduction gives primarily pinacol dianions through radical-radical, radical-ketone or ion-ketone coupling.[2] In the presence of proton donors such as acetic acid, two-electron (2-e) reduction also yields carbinols.[2g,3] The same reactivity pattern is demonstrated by pyridine-based aromatic ketones. For instance, one-electron (1-e) reduction of 4-acetylpyridine is followed by dimerization leading to the corresponding pinacol, while 2-e reduction at pH = 6.5 leads to methyl-4-pyridylmethanol.[4]

In contrast, pyridinium salts demonstrate chemically reversible electrochemical behavior upon reduction. Notable examples include the NAD^+/NADH couple that functions as an electron-transfer catalyst from flavoenzymes (iron-containing flavoproteins) to ATP in the respiratory chain,[5] and the various viologens (*N*,*N*′-diquaternized-4,4-bipyridinium salts).[6] The latter have been employed widely as redox mediators,[7] electrochromic materials,[8,9] electron acceptors in photoinduced electron transfers,[10] and redox probes in self-assembled monolayers,[11] dendrimers,[12] silicates,[13] zeolites,[14] and semiconductors.[15]

Significant attention has been focused also on the 1-e reduction of 4-acyl-, 4-carboxy-, 4-carbomethoxy-, 4-cyano- and 4-benzoylpyridinium cations, partly owing to the stability of the resulting radicals.[16] ESR spectroscopy, dipole moment considerations and chemical trapping experiments, point toward a pyridinium-localized radical as the 1-e reduced form of these cations.[17] For such radicals, possibilities for disproportionation have not been excluded,[18] and although coupling of 4-substituted pyridinium rings at the 4-position is generally considered sterically hindered, it has been observed; on the other hand, lack of coupling at the 2- and 6-positions has been difficult to reconcile.[19] Overall, the chemical stability and the intense color of the 1-e reduced form of 4-benzoylpyridinium cations has led to their consideration as inter- and intramolecular photoinduced electron-transfer acceptors,[16,20] and as electrochromic materials.[21] Owing to disproportionation,[18] however, the 1-e reduced form is expected to exist in equilibrium with low concentrations of the 2-e reduced species; therefore, the long-term survivability of the former depends on the chemical stability of the latter. In this context, a careful literature survey suggests that the generation and fate of the 2-e reduced form of this class of compounds is still lacking.

The present study comprises the first detailed investigation of the redox chemistry in CH_3CN of **1** and its analogues **2** and

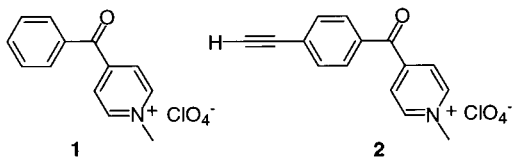

1

2

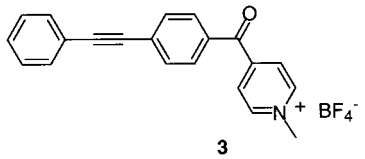

3

* To whom correspondence should be addressed.
† Phone: (573) 341-4391. E-mail: leventis@umr.edu.
‡ Phone: (573) 341-4353. E-mail: cslevent@umr.edu.

10.1021/jp0107199 CCC: $20.00
Published on Web 04/05/2001

3. The latter two compounds have been synthesized as models of **1** linked to conjugated systems for applications in molecular wires.

Our data shows that, in CH_3CN, 4-benzoyl-*N*-methylpyridinium salts possess a second *reversible* 1-e reduction wave which moves to more positive potentials in the presence of proton donors. On the basis of voltammetric and spectrophotometric evidence, this behavior, previously unknown for this class of compounds, is attributed to hydrogen bonding of the 2-e reduced forms with the proton donors, and is reminiscent of what is demonstrated by quinones in nonaqueous media.[22] In contrast to quinones, however, with weaker acids ($pK_a > 15$), and at time scales much longer than the time scale of the cyclic voltammetry, the hydrogen-bonded assemblages lead to proton transfer and eventual formation of *nonquaternized* 4-(α-hydroxybenzyl)pyridine and 4-benzoylpyridine. With acetic acid, proton transfer is faster, taking place within the time-scale of the cyclic voltammetry and leading to the *quaternized* 4-(α-hydroxybenzyl)-*N*-methylpyridinium cation. From a practical viewpoint, the important conclusion of this study is that if proton donors are meticulously excluded, 4-benzoylpyridinium salts can be used as reversible 1-e acceptors in lieu of either quinones or viologens.

2. Experimental Section

Methods. All electrochemical experiments were carried out at room temperature (23 ± 1 °C) with an EG&G 263A potentiostat controlled by the EG&G model 270/250 research electrochemistry software 4.30. Data were plotted using a Gateway 2000 computer and the Microcal Origin 4.1 software package. Cyclic voltammetry was conducted with an Au disk working electrode (1.6 mm in diameter, 0.0201 cm^2), and an aqueous Ag/AgCl reference electrode, both commercially available from Bioanalytical Systems, Inc., West Lafayette, IN. A Au foil (2.5 cm^2) was used as counter electrode. All cyclic voltammograms have been 80% compensated for the solution resistance. Our bulk electrolysis procedures have been described elsewhere.[23a] Here, bulk electrolysis was conducted in conjunction with NMR spectroscopy for identification of terminal products; for that purpose $NaClO_4$ was chosen as an NMR-silent supporting electrolyte. At the end of the electrolysis period, the contents of the working compartment of the H-cell were transferred in a pear-bottom flask, the solvent (CH_3CN/proton donor) was removed with a rotary evaporator, the solids were dried under vacuum, CD_3CN was added, and the NMR spectrum was recorded. Spectroelectrochemistry was conducted with a dual ITO-electrode thin-layer-cell as described before (cell thickness∼190 μm).[7a] All electrolytic solutions were degassed with N_2 or Ar.

All volumetric glassware was rinsed with acetone, washed with Micro™ cleaning solution in boiling water, rinsed with copious amounts of distilled water, and dried at 150 °C. The Au foil electrode was cleaned in a H_2O_2/c.H_2SO_4 (1:4 v/v) solution and oven-dried. All working electrodes were successively polished with 6, 3, and 1 μm diamond paste, washed with water and acetone, and then air-dried.

Anhydrous CH_3CN was purchased from Aldrich. Tetrabutylammonium perchlorate (TBAP) was used as a supporting electrolyte, and was prepared from an aqueous solution of tetrabutylammonium bromide (Aldrich) and 70% $HClO_4$. The resulting perchlorate precipitate was washed with copious amounts of deionized water (∼20 l), freeze-dried, recrystallized from methanol/ether, freeze-dried again and finally dried under vacuum at 80 °C.

For compound identification, ^1H and ^{13}C NMR spectra were obtained using a Varian INOVA 400 MHz NMR spectrometer, and are referenced versus TMS. Infrared spectra were recorded on a Nicolet Magna-IR model 750 spectrophotometer. GC−MS was done with a Hewlett-Packard Corp. model 5890 instrument, equipped with a J&W Scientific DB-5 MS column (3.0 m, O. D.=0.25 mm, i.d. = 0.25 μm) attached to a Hewlett-Packard Corp. mass selective detector (MSD) model 5972 (EI, scan mode), using helium as the carrier gas. UV−vis spectra were recorded with an Ocean Optics, Inc., model CHEM2000 miniature fiber optic spectrophotometer. Elemental analyses were performed by Oneida Research Services, Inc., Whiteboro, NY.

Electrochemical digital simulations were carried out on an iMac G3 Macintosh computer (64 MB RAM), using the Absoft Corporation FORTRAN 77 Compiler 4.4, as described elsewhere.[23a]

Materials. All starting materials and reagents were purchased from Acros or Aldrich and were used as received unless noted otherwise. All reactions were carried out under nitrogen in flame-dried glassware. Bromobenzene was washed consecutively with concentrated H_2SO_4, 10% NaOH, and H_2O followed by drying over $CaCl_2$ and vacuum distillation from sodium pellets using a glass helix packed column. Diisopropylamine was distilled from NaOH. Phenylacetylene was distilled through a vigreux column. Compound **1** was prepared as described before.[7b,23a]

4-(4-Bromobenzoyl)pyridine (4). Isonicotinic acid (15.012 g, 121.94 mmol) in thionyl chloride (50 mL) was stirred at 100 °C for 1.5 h. Excess $SOCl_2$ was removed under reduced pressure, and bromobenzene (80 mL) was added to the yellow residue. Upon cooling in an ice-bath, $AlCl_3$ (58 g, 0.43 mol) was added and the mixture was allowed to slowly return to room temperature. The solution was then heated to 90 °C and stirred for 4 h. The reaction was quenched by slowly pouring the reaction mixture into 400 mL of a 4.2% w/v HCl/ice−water solution. A pH = 4 was reached with the addition of Na_2CO_3 and then a saturated aqueous NaOH solution was added to attain pH ∼ 10. The organic layer was extracted with $CHCl_3$ and dried with $CaCl_2$. The solvents were removed with a rotary evaporator, and the crude product was loaded on a silica column (packed with hexane) and was eluted first with CH_2Cl_2 and then with CH_2Cl_2/CH_3OH, 49:1 v/v. Solvent removal yielded **4** as a white solid (28.4 g, 89%): mp 124−125 °C; ^1H NMR (400 MHz, $CDCl_3$) δ 8.83 (dd, J = 4.4 Hz, J = 1.6 Hz, 2 H), 7.68 (m, 4 H), 7.56 (dd, J = 4.4 Hz, J = 1.6 Hz, 2 H); ^{13}C NMR (100 MHz, $CDCl_3$) δ 193.98, 150.45, 143.79, 134.56, 131.98, 131.52, 128.82, 122.66; IR (KBr pellet) ν 3295 (w), 3100 (w), 3073 (w), 3019 (w), 1656 (s), 1582 (s), 1542 (m), 1420 (m) cm^{-1}; GC−MS *m*/*z* (rel intensity) 263 (M^+, 52), 261 (55), 185 (100), 183 (99), 157 (59), 155 (57), 76 (64), 51 (74).

4-(4-[(Trimethylsilyl)ethynyl]benzoyl)pyridine (5). Trimethylsilylacetylene (1.694 g, 17.25 mmol), dissolved in diisopropylamine (5 mL), was added to a solution of 4-(4-bromobenzoyl)pyridine (2.997 g, 11.43 mmol), dichlorobis(triphenylphosphine)palladium(II) (0.153 g, 0.218 mmol), and CuI (0.041 g, 0.22 mmol) in benzene (20 mL) and diisopropylamine (60 mL). After stirring overnight (14 h), the solvents were removed by rotary evaporation. The residue was passed through a column of silica gel (packed with hexane) using CH_2Cl_2 for elution. Two recrystallizations from hexane yielded light-brown transparent crystals: mp 85−87 °C; ^1H NMR (400 MHz, $CDCl_3$) δ 8.92 (br s, 2 H), 7.76 (m, 2 H), 7.58 (m, 4 H), 0.28 (s, 9 H); ^{13}C NMR (100 MHz, $CDCl_3$) δ 194.43, 150.57, 144.25,

135.33, 132.27, 130.13, 128.71, 123.05, 103.94, 99.13, −0.20; IR (KBr pellet) ν 3315 (w), 3066 (w), 2959 (m), 2905 (w), 2160 (s), 1656 (s), 1595 (s), 1555 (m), 1401 (s), 1280 (s) cm^{-1}; GC−MS *m*/*z* (rel intensity) 279 (M^+, 28), 264 (100).

4-(4-Ethynylbenzoyl)pyridine (6). The entire amount of **5** from above was dissolved in CH_3OH (80 mL) along with a catalytic amount of NaOH (0.027 g, 0.675 mmol). The solution was stirred at room-temperature overnight (14 h) and then poured into H_2O (115 mL). Diethyl ether (50 mL) and brine (100 mL) were added and the layers were separated. The aqueous layer was further extracted with diethyl ether (3 × 100 mL). The combined organic layers were dried with $MgSO_4$ and filtered. Rotary evaporation of the solvents left a solid which was sublimed at 100 °C under vacuum to yield **6** as white needles (1.91 g, 81% overall yield from **4**): mp 119−121 °C; ^{1}H NMR (400 MHz, CD_3CN) δ 8.78 (dd, J = 4.4 Hz, J = 1.6 Hz, 2 H), 7.8−7.6 (m, 4 H), 7.57 (dd, J = 4.4 Hz, J = 1.6 Hz, 2 H), 3.65 (s, 1 H); ^{13}C NMR (100 MHz, CD_3CN) δ 195.45, 151.40, 144.90, 136.92, 133.17, 131.10, 127.96, 123.67, 83.27, 82.48; IR (KBr pellet) ν 3300 (w), 3160 (s), 3046 (m), 2100 (s), 1660 (s), 1602 (s), 1548 (s), 1414 (s) cm^{-1}; GC−MS *m*/*z* (rel intensity) 207 (M^+, 46), 129 (100), 101 (51), 75 (33), 51 (48). Anal. Calcd for $C_{14}H_9NO$: C, 81.14; H, 4.38; N, 6.76. Found: C, 81.39; H, 4.48; N, 6.79.

4-(4-Ethynylbenzoyl)-*N*-methylpyridinium perchlorate (2). 4-(4-Ethynylbenzoyl) pyridine (1.914 g, 9.24 mmol) and CH_3I (5.327 g, 37.53 mmol) were dissolved in 50 mL CH_3CN. The mixture was stirred under reflux for 4 days while new portions of CH_3I (∼5 g, 0.04 mol) were added daily. At the end of the four-day period, the reaction mixture was cooled to room temperature, and diethyl ether was added to complete precipitation of the product which was then filtered and dried to yield 2.918 g, (90%) of crude 4-(4-ethynylbenzoyl)-*N*-methylpyridinium iodide as a light-orange solid. A portion of the product (1.451 g, 4.16 mmol) was dissolved in H_2O. Excess of 70% $HClO_4$ was added dropwise. The resultant off-white precipitate was recrystallized once from CH_3OH/Et_2O and once from H_2O to yield white crystals of **2** (0.901 g, 67%): ^{1}H NMR (400 MHz, CD_3CN) δ 8.81 (d, J = 6.4 Hz, 2 H), 8.17 (d, J = 6.4 Hz, 2 H), 7.80 (dd, J = 6.7 Hz, J = 2.0 Hz, 2 H), 7.70 (dd, J = 6.7 Hz, J = 2.0 Hz, 2 H), 4.39 (s, 3 H), 3.72 (s, 1 H); ^{13}C NMR (100 MHz, CD_3CN) δ 192.06, 152.45, 147.40, 135.20, 133.46, 131.32, 129.18, 128.19, 83.40, 82.98, 49.62; IR (KBr pellet) ν 3240 (s), 3135 (w), 3066 (m), 2173 (w), 2113 (w), 1675 (s), 1605 (s), 1575 (m), 1480 (m), 1400 (m) cm^{-1}. Anal. Calcd for $C_{15}H_{12}NO_5Cl$: C, 56.00; H, 3.76; N, 4.35. Found: C, 56.14; H, 3.63; N, 4.36.

4-(4-[(Phenyl)ethynyl]benzoyl)pyridine (7). Phenylacetylene (0.670 g, 6.56 mmol) was added dropwise to a stirred solution of **4** (1.148 g, 4.380 mmol), dichlorobis(triphenylphosphine)-palladium(II) (0.058 g, 0.083 mmol), and CuI (0.018 g, 0.094 mmol) in a 100 mL mixture of diisopropylamine and benzene (4:1, v:v). After stirring for 21 h, solvents were removed by rotary evaporation. The residue was extracted with CH_2Cl_2 and passed through a silica column (packed with hexane) using CH_2Cl_2 for elution. Recrystallization from $CHCl_3$ yielded **7** as a white solid (0.777 g, 63%): mp 147−148 °C; ^{1}H NMR (400 MHz, $CDCl_3$) δ 8.83 (dd, J = 4.4 Hz, J = 1.7 Hz, 2 H), 7.81 (dd, J = 6.8 Hz, J = 1.9 Hz, 2 H), 7.66 (dd, J = 6.8 Hz, J = 1.9 Hz, 2 H), 7.58 (dd, J = 4.4 Hz, J = 1.7 Hz, 2 H), 7.56 (m, 2 H), 7.37 (m, 3 H); ^{13}C NMR (100 MHz, $CDCl_3$) δ 189.99, 146.10, 139.90, 130.59, 127.46, 127.38, 125.78, 124.65, 124.52, 124.14, 118.43, 118.15, 89.07, 84.04; IR (KBr pellet): ν 3040 (w), 3019 (w), 2220 (m), 1649 (s), 1600 (s), 1595 (m), 1548 (m), 1500 (w), 1450 (w), 1400 (s) cm^{-1}; GC−MS *m*/*z* (rel intensity) 283(M^+, 68), 205 (100), 176 (84), 150 (41).

4-(4-[(Phenyl)ethynyl]benzoyl)-*N*-methylpyridinium tetrafluoroborate (3). $(CH_3)_3O^+BF_4^-$ (0.409 g, 2.77 mmol) dissolved in 10 mL CH_3NO_2 was added dropwise to a solution of 4-(4-[(phenyl)ethynyl]benzoyl)pyridine (0.502 g, 1.77 mmol) in CH_3NO_2 (60 mL) at room temperature. The solution was stirred for 20 min, and at the end of this period, the product was precipitated by addition of diethyl ether. The crude product was collected by vacuum filtration and recrystallized from water to yield **3** as a white solid (0.355 g, 52%): ^{1}H NMR (400 MHz, CD_3CN) δ 8.82 (d, J = 6.4 Hz, 2 H), 8.18 (d, J = 6.4 Hz, 2 H), 7.84 (dd, J = 6.7 Hz, J = 1.9 Hz, 2 H), 7.74 (dd, J = 6.7 Hz, J = 1.9 Hz, 2 H), 7.60 (m, 2 H), 7.45 (m, 3 H), 4.4 (s, 3 H); ^{13}C NMR (100 MHz, CD_3CN) δ 192.02, 152.79, 147.44, 134.72, 132.93, 132.75, 131.51, 130.47, 129.85, 128.28, 123.16, 118.36, 94.64, 89.00, 49.65; IR (KBr pellet) ν 3140 (w), 3110 (w), 3075 (w), 3066 (w), 2210 (w), 1667 (s), 1575 (w), 1480 (m), 1413 (m) cm^{-1}. Anal. Calcd for $C_{21}H_{16}NOBF_4$: C, 65.50; H, 4.19; N, 3.64. Found: C, 65.34; H, 3.94; N, 3.68.

4-(α-Hydroxybenzyl)pyridine (8).[24] Sodium borohydride (2.4 g, 63 mmol) was added to a solution of 4-benzoylpyridine (9.09 g, 49.6 mmol) in methanol (125 mL). The mixture was stirred at room temperature under nitrogen for 2 h. Methanol was then removed under reduced pressure and the solid was washed with 50 mL of water and dissolved in 200 mL of ethyl acetate. The water layer was extracted with two 50 mL portions of ethyl acetate. The ethyl acetate layers were combined and dried with sodium sulfate. Ethyl acetate was removed under reduced pressure, and the solid was triturated with hexane. The solution was filtered and the precipitate was dried in the vacuum oven at 40 °C overnight to give **8** (8.4 g, 91%): mp 120−122 °C; ^{1}H NMR (400 MHz, CD_3CN) δ 8.48 (dd, J = 1.6 Hz, J = 4.6 Hz, 2 H), 7.32 (m, 7 H), 5.76 (d, J = 3.6 Hz, 1 H), 4.11 (d, J = 3.6 Hz, 1 H); ^{13}C NMR (100 MHz, CD_3CN) δ 154.75, 150.61, 144.93, 129.55, 128.64, 127.57, 122.13, 74.92; IR (KBr pellet) ν 3400 (br, m), 3150 (br, s), 2825 (m), 1608 (s), 1562 (s), 1461 (s), 1414 (m), 1199 (m), 1051 (s), 1004 (s), 790 (m), 770 (s), 705 (s), 660 (s), 605 (s) cm^{-1}. Anal. Calcd for $C_{12}H_{11}NO$: C, 77.81; H, 5.99; N, 7.56. Found: C, 77.88; H, 6.03; N, 7.52.

4-(α-Hydroxybenzyl)-*N*-methylpyridinium tetrafluoroborate (10). Compound **10** was prepared following an identical preparative procedure to the one used for the synthesis of **3**: ^{1}H NMR (400 MHz, CD_3CN) δ 8.51 (d, J = 6.6 Hz, 2 H), 7.99 (d, J = 6.6 Hz, 2 H), 7.40 (m, 5 H), 6.01 (s, 1 H), 4.56 (br s, ^{1}H), 4.22 (s, 3 H); ^{13}C NMR (100 MHz, CD_3CN) δ 164.62, 146.00, 142.57, 129.94, 129.50, 127.91, 125.66, 74.26, 48.53.

3. Results

3.1. Synthesis of 1−3. Compounds **1**−**3** were prepared via quaternization of the corresponding free bases. 4-Benzoylpyridine, the free base of **1**, is available commercially, while **6** and **7** were synthesized via a common intermediate, 4-(4-bromobenzoyl)pyridine (**4**) (Scheme 1). Compound **4** was prepared from isonicotinic acid in two steps through a Friedel−Crafts acylation of bromobenzene with isonicotinoyl chloride, following standard procedures. $Pd(PPh_3)_2Cl_2$/CuI-catalyzed Heck-type coupling reactions between **4** and trimethylsilylacetylene or phenylacetylene gave **5** and **7**, respectively.[25] Compound **5** was deprotected to form the terminal alkyne, **6**, using a catalytic amount of NaOH in methanol. Methyl iodide is a commonly used quaternizing agent, but since the iodide salts of the 4-benzoylpyridinium cations considered here are not soluble in CH_3CN, metathesis to the corresponding perchlorates

SCHEME 1: Synthesis of 2 and 3

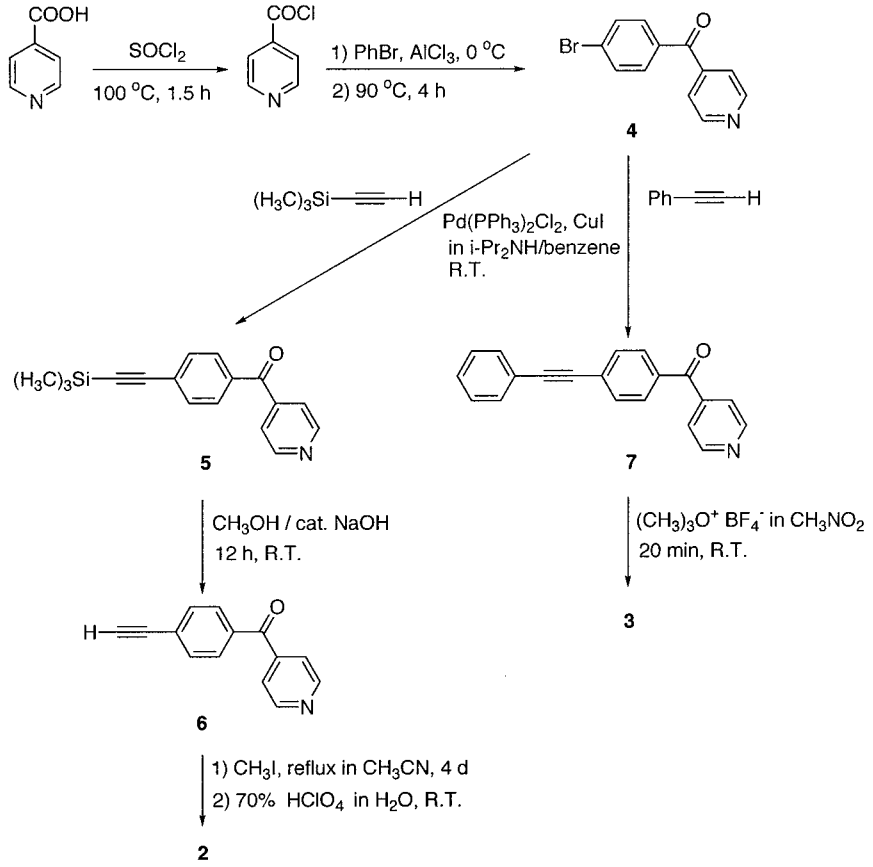

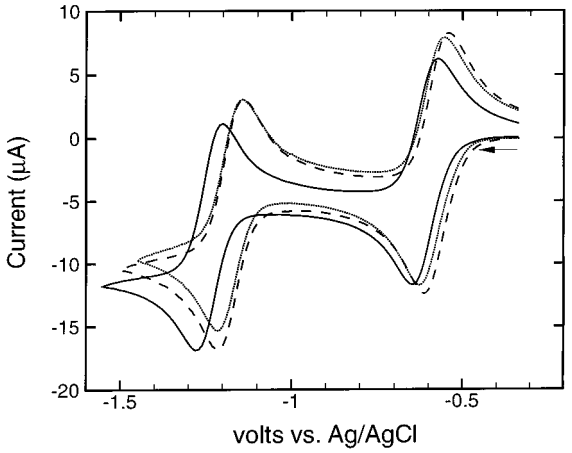

Figure 1. Electrochemical response at 40 mV/s of **1** (—, 2.82 mM), **2** (- - -; 2.89 mM), and **3** (• • •; 2.93 mM) in CH_3CN/0.5 TBAP using a Au disk electrode (0.0201 cm^2).

or tetrafluoroborates, which are both soluble in CH_3CN, is required. Alternatively, using trimethyloxonium tetrafuoroborate as the methylating agent yields directly the tetrafluoroborate salt and metathesis is not necessary.[26]

3.2. Electrochemical Reduction of 1−3. All initial redox characterization of compounds **1**−**3** was conducted in anhydrous CH_3CN, where they all demonstrate two well-separated 1-e reduction waves (Figure 1). The peak-to-peak separation (ΔE_{p-p}) in both waves is ~70 mV and rather insensitive to the potential sweep rate, at least in the range 40−120 mV/s. Table 1 summarizes the electrochemical data for compounds **1**−**3**.

Since the only other reference to a second electron reduction for this class of compounds reports that in aqueous electrolytes *N*-alkyl-4-benzoylpyridinium salts possess an irreversible second electron wave approximately 0.1−0.3 V more negative than the first,[21] it was deemed important to investigate the effect of different amounts of proton donors in the electrolytic solution.

TABLE 1: Redox Data for Compounds 1−3 Obtained with Cyclic Voltammetry in Anhydrous Acetonitrile[a]

compound	$E_{1/2}(1)$ (V)	$\Delta E_{p-p}(1)$ (mV)	$E_{1/2}(2)$ (V)	$\Delta E_{p-p}(2)$ (mV)
1	−0.626 ± 0.011	69 ± 3[b]	−1.260 ± 0.010	72 ± 4[b]
		70 ± 4[c]		73 ± 4[c]
2	−0.582 ± 0.005	70 ± 5[b]	−1.190 ± 0.010	74 ± 4[b]
		71 ± 4[c]		73 ± 6[c]
3	−0.592 ± 0.003	66 ± 2[b]	−1.188 ± 0.008	71 ± 3[b]
		71 ± 1[c]		73 ± 1[c]

[a] $E_{1/2}$'s are reported versus an aq Ag/AgCl reference electrode. [b] At 100 mV/s. [c] At 40 mV/s.

Perhaps not for obvious reasons, but intuitively of little surprise is the fact that the effect of proton donors on the redox chemistry of **1**−**3** depends on their chemical identity. The proton donors used in this study, and their pK_a values in water are presented in Table 2.

At concentrations up to 1.0 M, phenylacetylene does not have a significant effect on the voltammograms of **1**−**3**. The rest of the proton donors are separated into two groups: (Group I) *tert*-butyl alcohol (*t*-BuOH), 1-butanol (*n*-BuOH), H_2O, and CH_3OH; and (Group II) diethyl malonate, phenol, and acetic acid.

The common effect of the group I proton donors is demonstrated with **2** and methanol in Figure 2: as the concentration of CH_3OH increases, the first wave remains unaffected, while the second one moves to more positive potentials. The two waves retain their relative sizes and their peak-to-peak separations, meaning that both waves still correspond to 1-e reductions. However, as Figure 3 demonstrates, the relative effectiveness

TABLE 2: Proton Donors Used in This Study and Their pK_a Values toward Water

Ph-C≡CH	*t*-butanol	1-butanol	H_2O	CH_3OH	$CH_2(CO_2Et)_2$	phenol	CH_3CO_2H
23.2[27]	17[28a]	~16[28a]	15.74[28a]	15.2[28a]	13[28a]	9.9[29]	4.75[29]

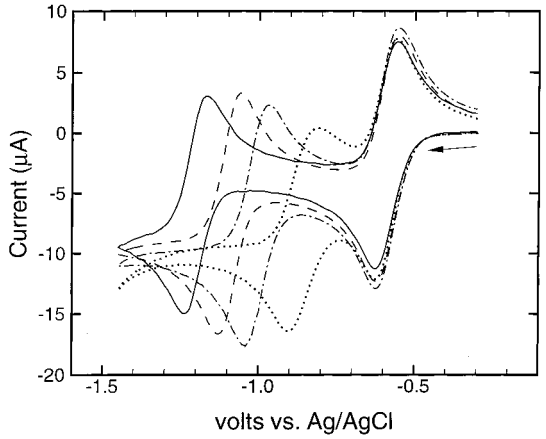

Figure 2. Electrochemical response of **2** (2.67 mM) at 40 mV/s in CH_3CN/0.5 M TBAP containing varying amounts of CH_3OH. (—) $[CH_3OH] = 0.0$ M, (- - -) $[CH_3OH] = 0.34$ M, (—•—) $[CH_3OH] = 1.44$ M, (• • •) $[CH_3OH] = 6.83$ M.

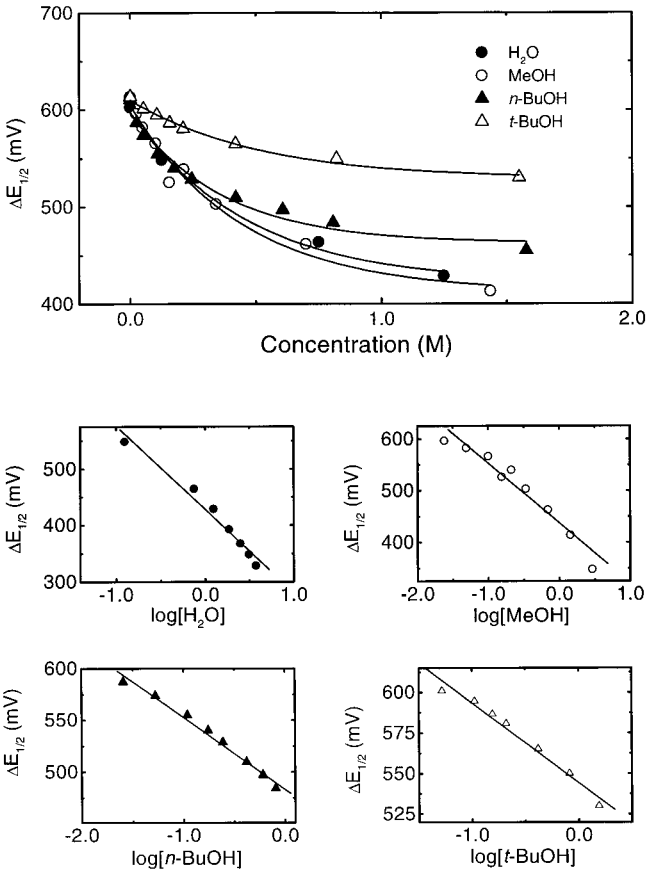

Figure 3. Cumulative results demonstrating the effect of varying the concentration of group I proton donors (H_2O, CH_3OH, *n*-BuOH, *t*-BuOH) on the position of the second electron reduction wave of **2**. Correlation coefficients ≥0.97. (Data obtained from experiments similar to those shown in Figure 2.)

of the group I proton donors in shifting the second wave closer to the first one is not the same, with H_2O or methanol being the most effective, and *t*-BuOH the least effective. All relevant data concerning **1**−**3** and group I proton donors are summarized in Table 3.

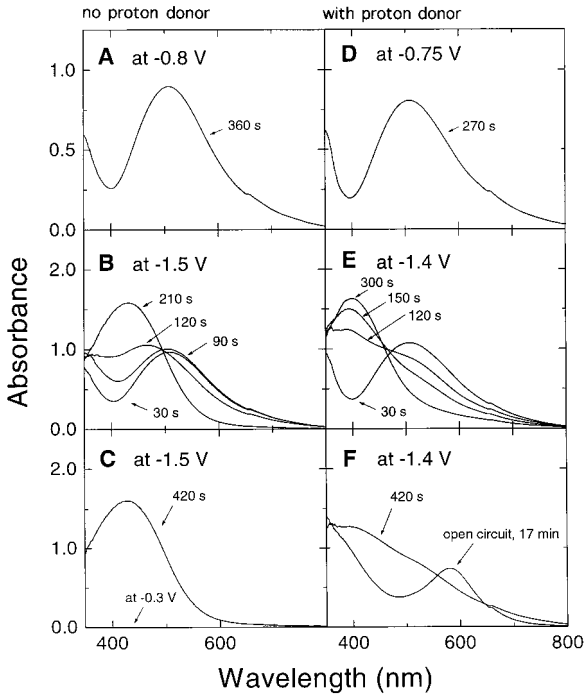

Figure 4. Spectroelectrochemistry of **1** (10 mM) using a dual ITO-electrode thin layer cell (~190 μm thick) in the absence (A−C) and in the presence (D−F) of 1.5 M of *n*-butanol.

More light is shed on the effect of group I proton donors on the redox chemistry of **1**−**3** by thin-layer-cell (TLC) spectroelectrochemistry. Figure 4 shows representative results obtained with **1** in the absence and the presence of a typical group I proton donor (*n*-BuOH), while all spectroelectrochemical data are summarized in Table 4. It is observed that the 1-e reduction of **1** in the absence or presence of group I proton donors yields practically identical absorption spectra with λ_{max}~507 nm (Figure 4A,D). The red species responsible for that absorption is stable for at least 20 min under inert atmosphere, and upon reoxidation at −0.3 V vs Ag/AgCl the colorless solution of **1** is recovered completely. Although cyclic voltammetry (Figure 2) suggests that both the one- and the two-electron reduction products of **1**−**3** are stable within the time-scale of cyclic voltammetry, spectroelectrochemistry now indicates that at least the 1-e reduction product of **1** does not pinacolize or react with group I proton donors even at much longer periods.

Reduction of **1** beyond its second wave (e.g., at −1.4 to −1.5 V vs Ag/AgCl) both with and without group I proton donors yields an early accumulation of the 1-e reduction product, which subsequently retreats in favor of the new absorbance corresponding to the yellow 2-e reduced form (Figure 4B,E). It is noted further that in the presence of the group I proton donors the λ_{max} of the 2-e reduction product is blue-shifted by about 32−34 nm relative to its absorption in the pure CH_3CN-based electrolyte. As will be defended below, that blue shift is consistent with a hydrogen bonding interaction between the 2-e reduced forms of **1**−**3** and the proton donors.

In the absence of a proton donor, the absorption spectrum of the 2-e reduction product does not decay, and the original colorless state is recovered completely by potentiostating the TLC at −0.3 V vs Ag/AgCl (Figure 4C). In the presence of group I proton donors, however, the spectrum of the 2-e reduced

TABLE 3: Slopes and Intercepts (both in mV) of the Plots of $\Delta E_{1/2}$ vs log[Proton Donor][a,b]

proton donor	H_2O		CH_3OH		*n*-BuOH		*t*-BuOH	
compound	slope	intercept	slope	intercept	slope	intercept	slope	intercept
1	-161 ± 1	455 ± 2	-100 ± 1	463 ± 2	-90 ± 1	489 ± 2	-50 ± 1	561 ± 1
2	-148 ± 1	428 ± 1	-117 ± 1	435 ± 2	-74 ± 1	478 ± 2	-48 ± 1	544 ± 1
3	-185 ± 2	442 ± 2	-106 ± 1	445 ± 3	-71 ± 1	467 ± 2	-51 ± 1	531 ± 1

[a] $\Delta E_{1/2} = E_{1/2}(1) - E_{1/2}(2)$. $\Delta E_{1/2}$ reports the position of the second wave, $E_{1/2}(2)$, with respect to the fixed position of the first one, $E_{1/2}(1)$. [b] Data comprise averages of two experiments at two different sweep rates (40 and 100 mV/s).

TABLE 4: Summary of Visible Absorption Data after One- and Two-Electron Reductions of 1 in the Presence of Group I Proton Donors[a]

	1-e reduction product	2-e reduction product
H-donor	λ_{max} (nm)	λ_{max} (nm)
none	506	429
H_2O	509	398
CH_3OH	509	395
n-BuOH	507	397

[a] [proton donor]=4.7 M.

species evolves slowly: for example in the presence of *n*-BuOH the absorbance with $\lambda_{max} = 397$ nm decays, and a new absorption feature with $\lambda_{max} = 584$ nm grows gradually (Figure 4F). That new feature increases even under open circuit conditions, and persists even after the thin layer cell is potentiostated back at -0.3 V. Nevertheless, that absorption feature begins to decay eventually, leading to a final pale-yellow solution with no distinct absorption features in the visible. Practically identical spectroelectrochemical results have been obtained in the presence of methanol. In the presence of water the absorption of the 2-e reduction product also decays slowly, but the transient absorption at ~580 nm is not observed. Generally, in the presence of group I proton donors, the 2-e reduction product reacts slowly toward terminal products having no distinct absorption in the visible. Separate bulk electrolyses of **1** at -1.4 V vs aq Ag/AgCl in the presence of 5 M of each of the group I proton donors reveal a surprisingly clean reaction: solvent removal and ^{1}H NMR spectroscopy of the residue in CD_3CN shows clearly two *nonquaternized* major terminal products, **8** and **9**:

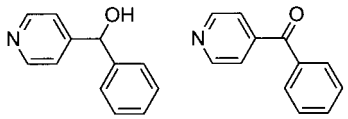

8 **9**

The structures of **8** and **9** were assigned by comparing their ^{1}H NMR signatures with those of authentic samples (the preparation of **8** is described in the Experimental Section, while **9** is commercially available). Fortuitously, the α-protons relative to the aromatic N-atom are more downfield than the other aromatic protons, and with the resolution of the 400 MHz NMR spectrometer they appear as a doublet in the quaternary salts and as a doublet of doublets in the free bases. Figure 5A shows representative ^{1}H NMR data in the region of the α-protons after electrolysis of **1** in the presence of 1-butanol. The two signals can be integrated, and the ratio of **8** to **9** is reported in Table 5. Figure 5B shows the results of a "control" experiment in which **1** was stirred with *t*-BuO^-K^+ in CD_3CN at room temperature (23 ± 1 °C) for 3 h; under these conditions, **1** reacts cleanly with the base producing **9**. Similar results have been obtained with **1** and CH_3ONa.

The electrochemical signature of the group II proton donors (diethylmalonate, phenol and acetic acid) is different, and is

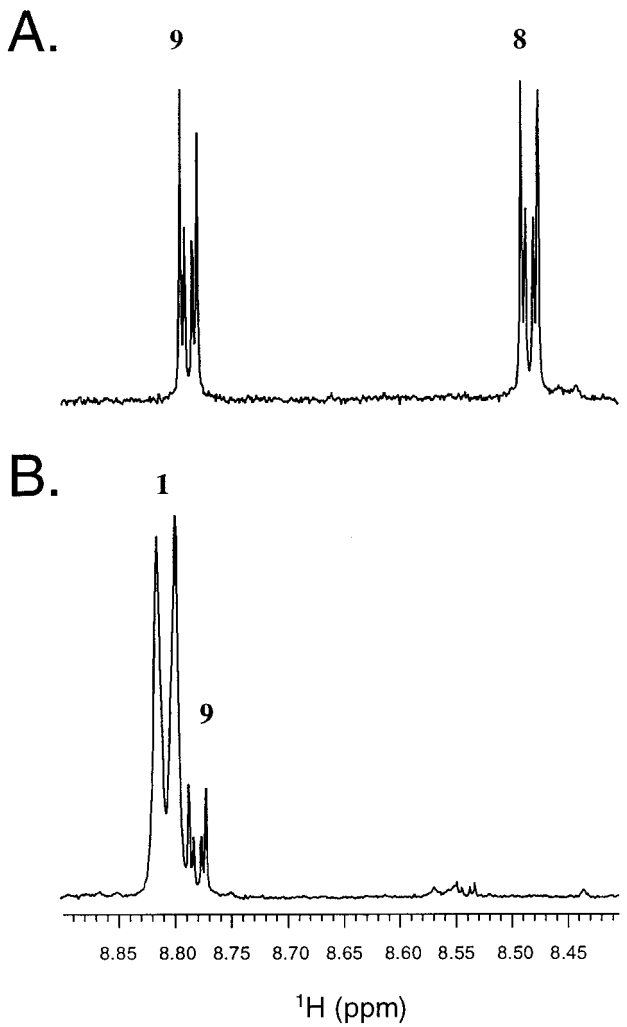

Figure 5. A. Typical ^{1}H NMR spectrum in CD_3CN of the product mixture after a 3 h electrolysis of **1** (3 mM) in CH_3CN/0.1 M $NaClO_4$ in the presence of 1-butanol (5 M). By comparison with part B of this Figure, no unreacted **1** has remained at the end of the electrolysis. B. ^{1}H NMR spectrum of the reaction mixture after **1** (3 mM) was stirred for 3 h at room temperature in CD_3CN in the presence of 3 mM *t*-BuO^-K^+. The signals correspond to the α-protons relative to the N-atom for each compound.

demonstrated in Figure 6. Here, only 0.5 mol-equivalent amount of the proton donor (dashed lines) versus **1** is enough to generate a new wave (marked with arrows) between the first and second electron reductions in the absence of proton donors (solid lines), while the original second wave is still present but its size has been diminished. Acetic acid, the stronger acid in the group, causes the most positive shift of the new intermediate wave. When the concentration of the group II proton donor increases to a 5 molar excess vs **1**, the original second-electron wave disappears completely, and the new wave is shifted to even more positive potentials (Figure 6, dotted lines). Again, that phenomenon is more pronounced with acetic acid than with phenol, which in turn is more effective than diethyl malonate. Specif-

TABLE 5: Terminal Product Ratios Relative to Unreacted Starting Material after 2-e Electrolytic Reductions of 1 in the Presence of Group I Proton Donors[a–c]

H-donor	[**1**]	[**8**]	[**9**]
H_2O	1	0	0.18
CH_3OH	0	0.44	1
n-BuOH	0	1	0.80
t-BuOH	0	0	1

[a] In all experiments, [**1**]=3.0 mM in CH_3CN/0.1 M $NaClO_4$, [proton donor] = 5 M, electrolysis time =3 h, applied potential=−1.4 V vs Ag/AgCl. The current decays to less than 5% of the original value in 15−20 min; the working electrode, however, was kept under potential control for the entire 3-h period. The product ratios were determined from data similar to those of Figure 5A. [b] A zero value means that the compound is undetectable by ^{1}H-NMR. [c] GC−MS analysis of the reaction mixture after electrolysis revealed no volatile products other than **8** and **9**.

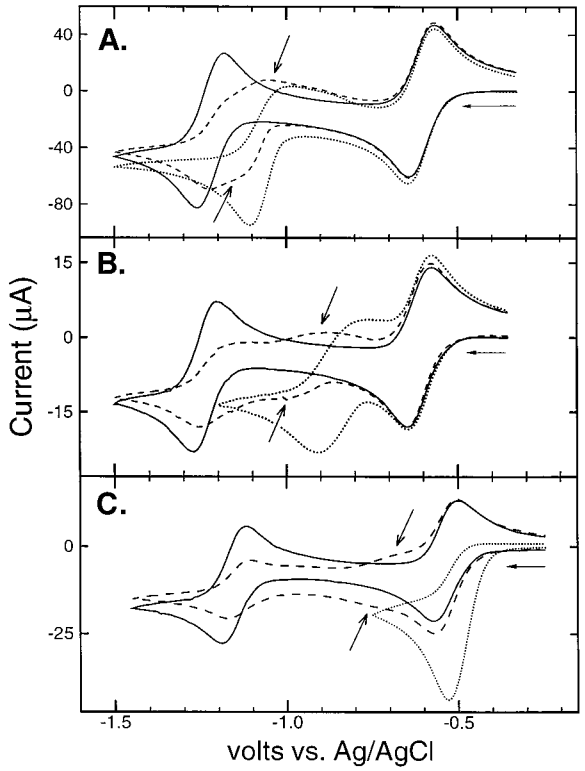

Figure 6. Electrochemical response of **1** at 100 mV/s in CH_3CN/0.5 M TBAP in the presence of of group II proton donors. (—) [HA] = 0.0 M, (- - -) [HA]/[**1**] = 0.5, (• • •): [HA]/[**1**] = 5. A: HA = diethyl malonate, [**1**] = 9.81 mM. B: HA = phenol, [**1**] = 3.02 mM. C: HA = CH_3CO_2H, [**1**] = 3.02 mM.

ically, with acetic acid as the proton donor, the new wave is so positive-shifted that it merges with the first one, which now represents an irreversible 2-e reduction (the current has doubled and the reoxidation wave has disappeared, Figure 6C). Increasing the potential sweep rate to 30 V/s, we have been able to regain some reversibility in the 2-e reduction of **1** in the presence of 5 molar excess of acetic acid (compare Figure 6C, dotted line, and Figure 7A).

TLC-electrolysis of **1** in the presence of 0.5 mol equiv amount of phenol after the first, second, and third waves produces absorption features corresponding respectively, (a) to the 1-e reduction product (λ_{max}=507 nm), (b) both the 1- and the 2-e reduction products (~507 nm and ~395 nm), and (c) a broader spectrum for the 2-e reduction product (λ_{max}~417 nm).

TLC-electrolysis of a 10 mM solution of **1** in the presence of ca. 50 mM of acetic acid does not produce any strong or

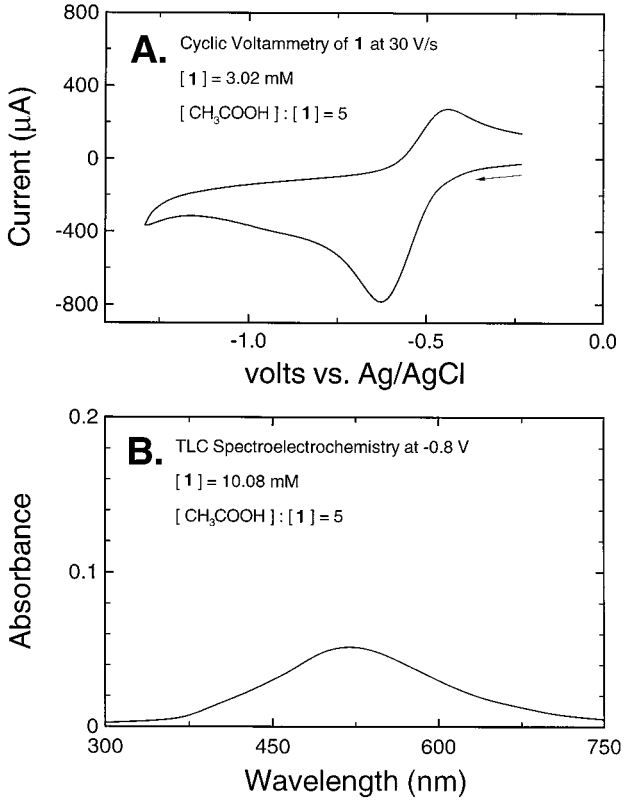

Figure 7. Data supporting a stepwise 2-e and 2-H transfer mechanism during the irreversible reduction of **1** in the presence of 5-molar excess of CH_3CO_2H. A: cyclic voltammetry of **1** (3.02 mM) at 30 V/s in CH_3CN/0.5 M TBAP in the presence of 15.07 mM of CH_3CO_2H. B. Spectroelectrochemical signature of **1** (10.08 mM) using a dual ITO electrode thin layer cell at −0.8 V vs Ag/AgCl in a CH_3CN/0.5 M TBAP solution containing 50.37 mM CH_3CO_2H. The spectrum was taken 3 min after the potential had been applied.

permanent absorption feature above 300 nm. Clearly, any intermediates react quickly and the terminal reduction product does not absorb in the visible. A weak transient absorption feature (λ_{max}~510 nm, $A \sim 0.05$, Figure 7B) corresponds to the 1-e reduction product of **1**. By comparison of the ^{1}H and ^{13}C NMR spectra of the reaction mixture from bulk electrolysis with the spectra of an authentic sample (see Experimental Section), 4-(α-hydroxybenzyl)-*N*-methylpyridinium cation (**10**) was identified as the only terminal product from the reduction of **1** in the presence of a 5 M excess of acetic acid. (After a 3 h electrolysis, ^{1}H NMR analysis showed only two compounds present: **1** and **10**; [**1**]/[**10**] = 1.06.)

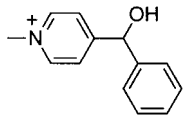

10

4. Discussion

Although reports involving benzoylpyridinium salts are scarce,[20,21,30] benzoylpyridines, themselves have been investigated for their potential pharmacological properties,[31] and have been synthesized via reaction of cyanopyridines with phenyl Grignard reagents,[31b–d] Friedel−Crafts reactions of nicotinoyl chlorides with substituted benzenes,[31a,d,f,g,32] and by the oxidation of benzylpyridines or 1-phenyl-1-pyridylmethanols with potassium permanganate or chromic acid.[31g,33]

The synthetic procedure of Scheme 1 was selected because both **2** and **3** emerge from the common intermediate **4**. Alternatively, **3** can be prepared via a $Pd(PPh_3)_2Cl_2$/CuI-catalyzed coupling of bromobenzene with **6**, which in turn can be synthesized from the reaction of 4-vinylphenylmagnesium bromide with 4-cyanopyridine followed by acid hydrolysis,[28b] bromination of the double bond, and dehydrohalogenation. This procedure, however, is lengthier and the yield of **6** is very low (<10%), probably due to polymerization of the Grignard reagent.[34]

Within the time-scale of cyclic voltammetry and in the presence or absence of group I proton donors, **1**−**3** undergo two sequential, chemically reversible ($i_{p,c}/i_{p,a} \approx 1 \pm 0.05$ for both waves), 1-e reductions. The ΔE_{p-p} values of both waves of all three compounds are practically independent of the potential sweep-rate, indicating reversibility. Therefore, in the ensuing discussion the cyclic voltammetric half-wave potentials, $E_{1/2}$, of both reduction waves are assumed to correlate with the concentrations of the involved species via the Nernst equation.

In the absence of proton donors, the redox chemistry of **1**−**3** (X = H−, H−C≡C−, and Ph−C≡C−) is described by eqs 1 and 2. The two possible 1-e reduced products, **11** and **11a**, are not canonical forms: **11** is a nonaromatic neutral species, while the zwiterionic radical **11a** is the typical 1-e reduction product expected from a ketone.

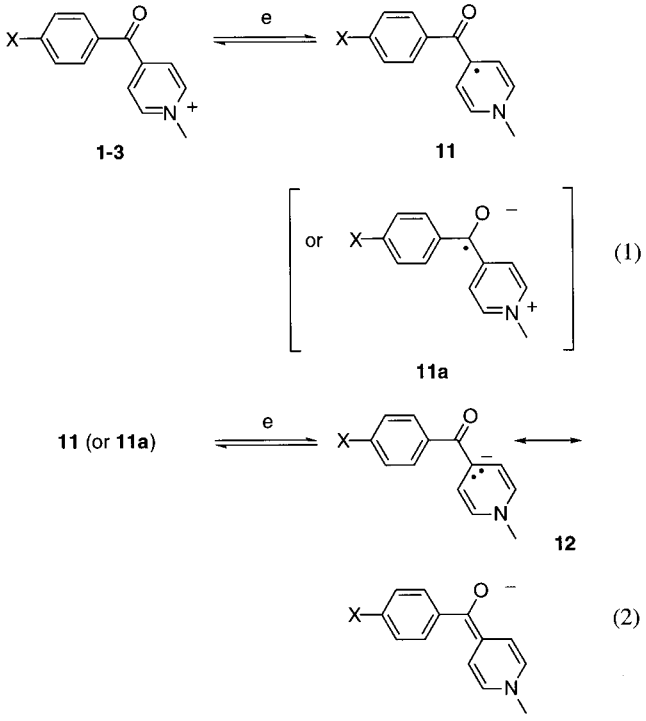

Both isomers **11** and **11a** yield the same ionic species **12** by a second electron reduction. According to the literature, the nature of the 1-e reduced form of other 4-substituted pyridinium salts conforms to an **11**-type structure.[17] It is also noteworthy that in analogy to **11a** the 1-e reduction product of 4-acetylpyridine leads to pinacolization,[4] while the 1-e reduction of the 4-acetyl-*N*-methylpyridinium cation leads only to coupling in the 4-position relative to the aromatic nitrogen, obviously via a radical analogous to **11**.[19] In this realm, our spectroelectrochemical data show that the chemical stability of the 1-e reduced form of **1** extends well beyond the time-scale of the cyclic voltammetry, and structure **11** provides an adequate explanation for both the lack of pinacolization and the lack of coupling due to steric hindrance. Furthermore, by comparative analysis of the cyclic voltammograms of **2** and **3** with respect to **1** (Figure 1), the position of the second wave is more sensitive to substitution than that of the first one. This indicates, on the basis of the Hammett-type of argumentation,[28c] that the first electron goes into the pyridinium ring, while the second electron generates a negative charge on the carbonyl group, which is closer to the point of substitution.

Spectroelectrochemistry provides further understanding for the redox chemistry of **1**−**3** by showing clear evidence for a homogeneous comproportionation reaction between **12** and **1** producing **11**, according to eq 3. Although the red 1-e reduction product, **11**, is incompatible with the electrode held at potentials

$$\mathbf{12} + \mathbf{1} \longleftrightarrow 2\ \mathbf{11} \qquad (3)$$

beyond the second reduction wave (e.g., at −1.5 V vs Ag/AgCl, Figure 4B), nevertheless it is still produced transiently on the way to yellow **12**. Also, the similar spectral evolution of Figures 4B and E suggests that comproportionation reactions proceed unobstructed, and **11** is formed irrespective of the chemical identity of the 2-e reduced form in the absence or presence of group I proton donors.

Group I proton donors shift positive only the second reduction waves of **1**−**3**, in a way that depends on their chemical identity and concentration (Figure 3 and Table 3). According to the literature, analogous behavior has been encountered with quinones in nonaqueous media, and has been debated for decades; it was recognized early that an ECE type mechanism (initial electron transfer, E, followed by a homogeneous chemical reaction, C, and a second electron transfer, E) had to be excluded, because it would affect the position and the shape of both waves.[35] Subsequently, attention was focused on an EEC type of mechanism, but the older literature commonly implied that a direct proton transfer was involved immediately after the second electron reduction. If that model was to be adopted for explaining the positive shift of the second wave of **1**−**3** in the presence of group I proton donors, it would involve protonation of **12** according to eq 4. However, digital simulations show that eq 4 introduces chemical irreversibility in both waves, and that has been traced to the limited supply of A^-, which is produced

$$\mathbf{12} + \mathrm{m\ HA} \longleftrightarrow \text{protonated-}\mathbf{12} + \mathrm{m\ A^-} \qquad (4)$$

and consumed via eq 4. It is thereby concluded that in order for eq 4 to keep the supply of **12** at the level demanded by eq 2, a large excess of A^- should be present in the electrolytic solution at all times.

It is evident that in order to preserve the reversibility of both waves of **1**−**3** and explain the positive shift of $E_{1/2}(2)$ in the presence of group I proton donors, the interaction between **12** and the proton donors should not produce the conjugate base A^-. In this context, comparison of the spectroelectrochemical data of Figures 4B and E suggests development of hydrogen bonding between **12** and the group I proton donors: the blue-shifted absorption of the 2-e reduction product in the presence of the group I proton donors, indicates that the HOMO of **12** has been stabilized by about 5.4 kcal/mol, which is a typical value for a hydrogen bonding interaction.[28d] (In contrast, the absorption spectrum of **11** is not affected by the presence of group I proton donors: see Table 4 or compare Figures 4A and D.) From a purely voltammetric perspective, it has been proposed that hydrogen bonding between proton donors and the oxygen of a carbonyl group renders the latter more easily reducible and creates polarographic prewaves in the electrochemical reduction of ketones.[36] Hydrogen bonding has been

considered also between phenol and the 1-e reduction product of 1-hydroxy-9,10-anthraquinone as a possible explanation for a new polarographic wave (between the two original ones) in the presence of a stoichiometric amount of phenol.[35d] However, digital simulations show that *any* interaction of the 1-e reduced form affects the position and slope of both waves, leaving the 2-e reduced form as the only candidate for developing hydrogen bonding that would affect the position of only the second wave. In this regard, the electrochemistry of quinones was revisited recently by Cupta et al., who introduced hydrogen bonding into digital simulations in order to explain their voltammetry in nonaqueous media.[22]

Accepting that only the 2-e reduced forms of **1**−**3** develop hydrogen bonding with the group I proton donors, there are four possible mechanisms explaining the positive shift of the second wave. **12**--HA^m represents the hydrogen-bonded adduct

Mechanism I

$$m\ HA \underset{}{\overset{K'}{\rightleftharpoons}} HA^m$$

$$\mathbf{1} + e \rightleftharpoons \mathbf{11}$$

$$\mathbf{11} + e + HA^m \rightleftharpoons \mathbf{12}\text{--}HA^m$$

Mechanism II

$$m\ HA \overset{K'}{\rightleftharpoons} HA^m$$

$$\mathbf{1} + e \rightleftharpoons \mathbf{11}$$

$$\mathbf{11} + e \rightleftharpoons \mathbf{12}$$

$$\mathbf{12} + HA^m \overset{K''}{\rightleftharpoons} \mathbf{12}\text{--}HA^m$$

Mechanism III

$$\mathbf{1} + e \rightleftharpoons \mathbf{11}$$

$$\mathbf{11} + e + m\ HA \rightleftharpoons \mathbf{12}\text{--}HA^m$$

Mechanism IV

$$\mathbf{1} + e \rightleftharpoons \mathbf{11}$$

$$\mathbf{11} + e \rightleftharpoons \mathbf{12}$$

$$\mathbf{12} + m\ HA \overset{K}{\rightleftharpoons} \mathbf{12}\text{--}HA^m$$

of **12** to either "*m*" molecules of HA or a *m*th member aggregate of HA (HA^m). Mechanisms I and II assume preassociation of the proton donors in aggregates, and should become important at higher concentrations of HA. In relatively dilute solutions of HA, mechanisms III and IV are expected to predominate. For example, if HA = H_2O, Bertie et al. have reported that when the mole-fraction of water in acetonitrile is less than ~0.15 (or [H_2O] < ~3 M), there are "enough CH_3CN molecules to surround each water molecule, and the water molecules increasingly form just a single hydrogen bond to one of the surrounding CH_3CN molecules."[37] Mechanism III is a limiting case of mechanism IV for very fast establishment of the equilibrium between **12** and HA. Digital simulations (Figure 8) provide supporting evidence for both mechanisms by showing that mechanism III for example, is fully capable of reproducing the main facets of Figures 2 and 3, and Table 3; namely that, in the presence of an associative interaction (e.g., hydrogen bonding) between **12** and HA, the first wave remains unchanged, whereas the second one moves to more positive potentials with (a) increasing concentration of HA and (b) increasing number of HA molecules entering the association. Now, which one of the two mechanisms, III or IV, is actually the correct one is decided as follows.

According to mechanisms III and IV, the relationship between the electrode potential, *E*, and the ratio of the electrode-surface concentrations, [**11**]/[**12**--HA^m], along the second wave are given at 25 °C by eqs 5 and 6, respectively, where $E_{1/2}°(2)$ is the half-wave potential of the second wave in the absence of HA.

$$E = E_{1/2}°(2) + m\ 0.059 \log[\mathrm{HA}] + 0.059 \log[[\mathbf{11}]/[\mathbf{12}\text{--}\mathrm{HA}^m]] \quad (5)$$

$$E = E_{1/2}°(2) + 0.059 \log K + m\ 0.059 \log[\mathrm{HA}] + 0.059 \log[[\mathbf{11}]/[\mathbf{12}\text{--}\mathrm{HA}^m]] \quad (6)$$

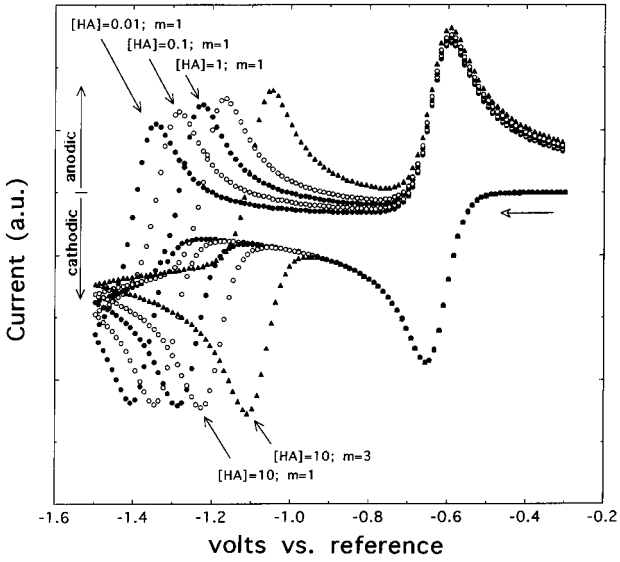

Figure 8. Digital simulations demonstrating the effect of [HA] and of "*m*" on the cyclic voltammetry of a redox-active species (0.001 M) reacting according to mechanism I. [HA] is in M. The simulations were conducted using an iteration time interval of 1 ms. The diffusion coefficients of all three redox states were assumed equal so the cyclic voltammograms are undistorted by the homogeneous comproportionation reaction between the redox-active species and its 2-e reduced form.[23]

On the basis of eqs 5 and 6, the value of $E_{1/2}(2)$ in the presence of HA is given for mechanisms III and IV by eqs 7 and 8, respectively.

$$E_{1/2}(2) = E_{1/2}°(2) + m\ 0.059 \log[\mathrm{HA}] \quad (7)$$

$$E_{1/2}(2) = E_{1/2}°(2) + 0.059 \log K + m\ 0.059 \log[\mathrm{HA}] \quad (8)$$

According to eqs 7 and 8, $E_{1/2}(2)$, irrespective of mechanism, should vary linearly with log[HA], and the slope should depend on the number of HA molecules participating in the **12**- -HA^m assemblages. The same argument has been advanced by Ravenga et al. for the redox behavior of anthraquinone in aqueous media,[35f] and by Cupta et al. for the electrochemistry of quinones in nonaqueous media.[22] If mechanism III is correct, the intercept of $\Delta E_{1/2}$ vs log[HA] should be independent of the identity of the acid, while the opposite should be valid if mechanism IV is correct. In fact, the subtle difference between mechanisms III and IV is that in the latter, the shift of the $E_{1/2}(2)$ depends also on the equilibrium constant, K, of the interaction of **12** with HA. That equilibrium constant depends on the tendency of HA to form hydrogen bonding, which in turn depends on the polarization of the H−A bond, and therefore is related to the acidity of the proton donor. In conclusion, if mechanism IV is correct, the acid strength should play an important role in the positive shift of the second wave.

According to Figure 3 and Table 3, the slope of $\Delta E_{1/2}$ vs the log[HA] varies with the identity of the group I proton donor, and for compound **3** for example, the values of the slope are 0.86, 1.2, 1.8 and 3.1 times 0.059 V for *tert*-butyl alcohol, *n*-butanol, CH_3OH, and H_2O, respectively. Because these multiples of 0.059 V represent the *average* number of HA molecules associated with **12** in **12**--HA^m, this trend most probably reflects the relative size of the proton donors around the O-atom. Structures **12a**−**c** illustrate the hydrogen bonded associations of the 2-e reduced forms of **1**−**3**, following a first

significant figure approximation for the participating number of HA molecules.[38]

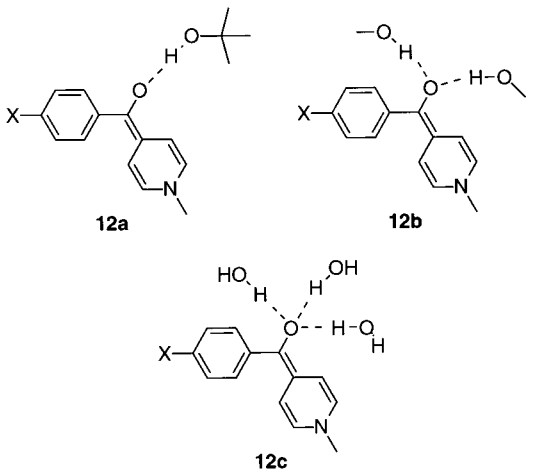

The intercepts of the plots of $\Delta E_{1/2}$ vs log[H_2O] and log[CH_3OH] are numerically close (Table 3), but the intercepts with *n*- and *tert*-butyl alcohol are progressively higher. The equilibrium constants for the formation of the various **12**--HA^m adducts are calculated from the intercepts (Table 3) and the $E_{1/2}°(2)$ values (Table 1) via eq 9. For compound **1**, for example, it is calculated

$$\text{intercept} = E_{1/2}°(2) + 0.059 \log K \qquad (9)$$

that $K_{\mathbf{12}-(t-\text{BuOH})^1} = 17\ M^{-1}$, $K_{\mathbf{12}-(n-\text{BuOH})^1} = 2.9 \times 10^2\ M^{-1}$, $K_{\mathbf{12}-(\text{CH}_3\text{OH})^2} = 7.9 \times 10^2\ M^{-2}$, and $K_{\mathbf{12}-(\text{H}_2\text{O})^3} = 1.08 \times 10^3\ M^{-3}$. These equilibrium constants increase as the acid strength of the group I proton donor increases (Table 2), supporting mechanism IV.

A correct mechanism should be also consistent with the data obtained with group II proton donors. Indeed, being stronger acids, group II proton donors shift the second wave much more effectively than their group I counterparts (compare Figures 2 and 6). Therefore, to monitor the effect of all three group II proton donors it was necessary to work with sub-mol equivalent amounts relative to **1**−**3**. But then, there is stoichiometrically not enough group II proton donor for all molecules of **1**−**3** to associate with, and therefore the original second waves survive (albeit reduced in size—Figure 6, dashed lines) while a new wave appears between the two old ones. The $E_{1/2}$'s of the new intermediate waves correlate well with the pK_a's of the three group II proton donors (Figure 9), supporting their origin from a hydrogen bonding interaction of **12**, in analogy to the inferences in conjunction with mechanism IV and the group I proton donors. The conclusions based on the voltammetric data are also consistent with the spectroelectrochemical data obtained with 0.5 mol-equivalent amount of phenol relative to **1**, showing the coexistence of **11** with **12**--HA^m after the new intermediate wave, and of **12** with **12**--HA^m after the original second wave.

Finally, it is noted that with only a moderately higher concentration of CH_3CO_2H relative to **1**, the second wave merges with the first one, becoming an irreversible 2-e wave (Figure 6C, dotted line). Bulk electrolysis under these conditions at −0.8 V vs Ag/AgCl yields only one product, the colorless 4-(α-hydroxybenzyl)-*N*-methylpyridinium cation (**10**). Formation of **10** requires transfer of two electrons and two protons. The question whether the protons are transferred concurrently or sequentially with the electrons, is addressed as follows. Both the partial reversibility during cyclic voltammetry at 30 V/s (Figure 7A) and the low transient absorbance of **11** during TLC

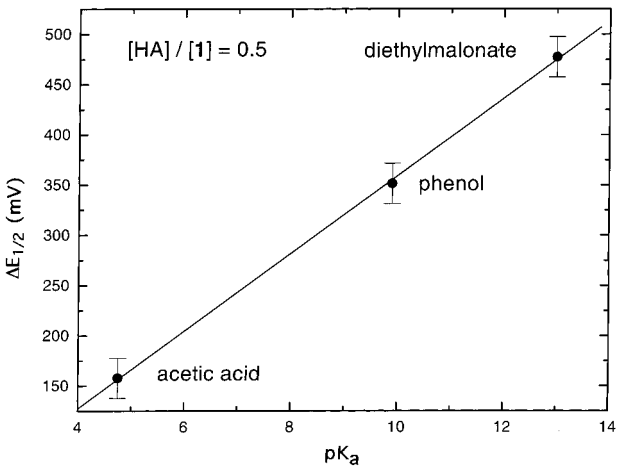

Figure 9. Linear correlation of the $\Delta E_{1/2}$ [$=E_{1/2}(1) - E_{1/2}(2)$] values of **1** vs the pK_a values of group II proton donors. $E_{1/2}(2)$ refers to the $E_{1/2}$ value of the new wave that appears between the original waves when [HA]/[**1**] = 0.5 (refer to Figure 6).

electrolysis of **1** at −0.8 V in the presence of a 5-molar excess of CH_3CO_2H (Figure 7B), support the fact that the 2-e and the 2-H transfer do not take place concurrently, but sequentially. If **10** was formed via a simultaneous 2-e/2-H transfer, the 2-e reduction wave of **1** in the presence of 5-molar excess of CH_3CO_2H would not show any signs of chemical reversibility at any sweep rate, because **10** is not oxidizable in the range between −1.5 and 0 V vs Ag/AgCl. Furthermore, under 2-e transfer conditions, **11** can only be produced via the comproportionation reaction of **1** with the 2-e reduction product or its hydrogen-bonded form (eq 3). Therefore, if protons and electrons were transferred concurrently, **11** should be produced from the reaction of **1** with **10**; but as it was stated, **10** is not oxidizable between −1.5 and 0 V, so its reaction with **1** is not favored thermodynamically. Based on the above, the most probable mechanism for the reduction of **1**−**3** in the presence of acetic acid is described by eqs 10−13. Equations 10 and 11 leave the possibility open for (a) a large positive shift of the second wave by hydrogen bonding so that it merges with the first (Figure 6C), (b) some electrochemical reversibility at higher sweep rates (Figure 7A), and (c) a comproportionation reaction that generates **11** transiently (Figure 7B). In this realm, eq 12 suggests that **12**--HA^m is capable of comproportionation with **1** (a fact also supported by the spectroelectrochemical data in the presence of *n*-BuOH—compare Figure 4B and E), while eq 13 describes the irreversible formation of **10** from **12**--$HOCOCH_3^m$ via a 2-H transfer.

$$\mathbf{1} + 2\,e \;\rightleftharpoons\; \mathbf{12} \qquad (10)$$

$$\mathbf{12} + m\,CH_3CO_2H \;\rightleftharpoons\; \mathbf{12}\text{--}HOCOCH_3^m \qquad (11)$$

$$\mathbf{12}\text{--}HOCOCH_3^m + \mathbf{1} \;\rightleftharpoons\; 2\,\mathbf{11} + m\,CH_3CO_2H \qquad (12)$$

$$\mathbf{12}\text{--}HOCOCH_3^m \longrightarrow \mathbf{10} + 2\,CH_3CO_2^- + (m-2)\,CH_3CO_2H \qquad (13)$$

Finally, the last issue to be addressed is the different product distribution upon electrolysis of **1**−**3** in the presence of group I proton donors vs CH_3CO_2H. Bulk electrolysis of **1** in the presence of group I proton donors yields *only* nonquaternized terminal products (compounds **8** and **9**). No trace of **10** was ever detected among the electrolysis products in the presence of group I proton donors, and no trace of either **8** or **9** was ever detected in the presence of CH_3CO_2H. The immediate question is whether **9** is formed from **8** or vice versa. As it was mentioned in the beginning of this section, alcohols analogous to **8** can be

oxidized to the corresponding ketones (compounds analogous to **9**) only with strong oxidizing agents such as $KMnO_4$ or chromic acid.[31g,33] Therefore, **9** cannot be formed from **8** in the reducing environment during bulk electrolysis. On the other hand, the first-electron reduction of **9** has $E_{1/2} = -1.47$ V vs Ag/AgCl,[20] but in analogy to 4-acetylpyridine,[4] the 1-e reduced form of **9** is expected to pinacolize, and not to form **8**. No trace of such pinacol has been detected by ^{1}H NMR among our electrolysis products, so the reduced form of **9** was not present during the electrolytic formation of **8**. All in all, **8** and **9** are formed independently of one another, and **9**, being an oxidized form, is probably formed from unreacted **1** after the three-hour long electrolytic experiment is ended.

Indeed, spectroelectrochemistry shows that in the presence of group I proton donors the irreversible reaction of **12**--HA^m toward terminal products is slow (Figure 4F). As soon as the reducing environment is removed, the remaining **12**--HA^m is expected to be converted back to **1**, owing to the reversibility of the voltammetric second wave in the presence of group I proton donors (Figure 2). According to the control experiment of Figure 5B, once **1** is formed, it reacts with alkoxide leading to dequaternization and formation of **9**. (A literature survey shows that nucleophile-induced dequaternization of pyridinium salts is known but perhaps the full latitude of this reaction may not have been appreciated.[39]) The next question is related to the origin of the alkoxide in the electrolytic solution. This is not difficult to reconcile: **8** must be produced from **12**--HA^m via a two-step proton transfer (eqs 14 and 15), whose side

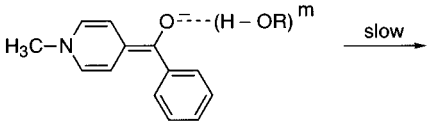

12---HA^m (HA = ROH or H_2O)

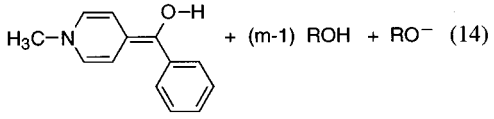

13

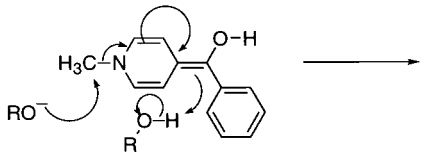

13

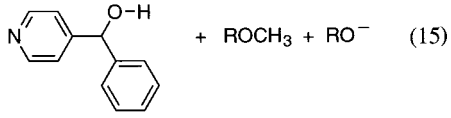

8

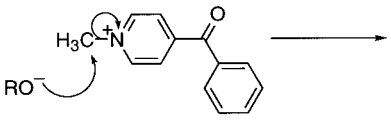

1

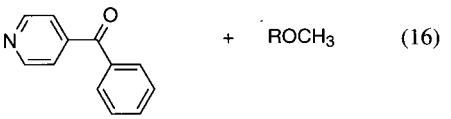

9

product should be an alkoxide (or HO^-). Stronger nucleophiles, such as CH_3O^- and *n*-BuO^-, react with intermediate **13** according to eq 15 giving **8** (Table 5), while all four conjugate bases of the group I proton donors react with **1** produced at the end of the electrolysis by air oxidation of either **13**, or unreacted **12**- -HA^m, to give **9** (eq 16).[40]

In the presence of CH_3CO_2H and in analogy to eq 14, **12**--(HOCOCH$_3$)^m should first yield **13** and $CH_3CO_2^-$. Owing not only to the stronger acidity of CH_3CO_2H relative to the group I proton donors, but also to the weaker nucleophilicity of $CH_3CO_2^-$ compared to HO^- and RO^-, **13** follows a different reaction pathway as shown by eq 17.

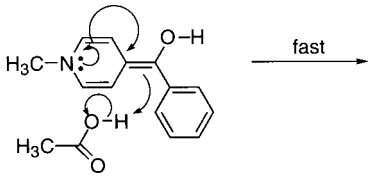

13

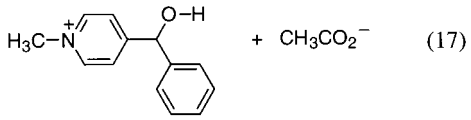

10

5. Conclusions

It has been reported for the first time that in nonaqueous CH_3CN, 4-benzoyl-*N*-methylpyridinium cations, such as **1**−**3**, undergo two successive well-separated 1-e reductions, in analogy to viologens and quinones. The chemical inertness and the intense color of the 1-e reduced forms, **11**, suggest that **1**−**3** could be considered for applications as redox mediators or electrochromic compounds. Although the 2-e reduction of 4-benzoyl-*N*-methylpyridinium cations has not been studied before, nevertheless it has been recognized that **12** could exist in equilibrium with **11**, according to the disproportionation reaction of eq 18.[18] Due to the wide separation of the two

$$2\ \mathbf{11} \rightleftharpoons \mathbf{1} + \mathbf{12} \qquad (18)$$

reduction waves of **1**−**3** (Table 1), the room-temperature equilibrium constant of eq 18 in the absence of a proton donor is calculated equal to 2×10^{-11}. Therefore, the equilibrium concentration of **12** (and also of **1**) in a 3 mM solution of **11** is 1.27×10^{-5} mM. In the presence of water or alcohols, however, the second wave moves closer to the first one, hence the equilibrium constant of eq 18 increases significantly. This fact, in conjunction with the eventual reaction of **12** with the group I proton donors, might limit applications where the **1**/**11** redox couple should be able to survive millions of cycles for very long periods of time (in the order of years) as in certain electrochromic devices.[42] In this regard, the results presented here suggest that under rigorous exclusion of proton donors such extended operational lifetimes may be possible.

Acknowledgment. We gratefully acknowledge support from The Petroleum Research Fund, (administered by the ACS, Grant 35154-AC5), and from the University of Missouri Research Board. We thank Dr. D. Hasha of the University of Missouri—Rolla for his assistance with NMR and Dr. M. Komarynsky of Washington University in St. Louis for his assistance with the H-cell.

References and Notes

(1) Feoktistov, L. G. In *Organic Electrochemistry*; 2nd ed.; Baizer, M. M., Lund, H., Eds.; Marcel Dekker: New York, 1983; p 315.

(2) (a) Stocker, J. H.; Jenevein, R. M.; Kern, D. H. *J. Org. Chem.* **1969**, *34*, 2810. (b) Rudd, E. J.; Conway, B. E. *Trans. Faraday Soc.* **1971**, *67*, 440. (c) Nadjo, L.; Saveant, J. M. *J. Electroanal. Chem.* **1973**, *44*, 327. (d) van Tilborg, W. J. M.; Smit, C. J. *J. R. Neth. Chem. Soc.* **1979**, *98*, 532. (e) Swartz, J. E.; Mahachi, T. J.; Kariv-Miller, E. *J. Am. Chem. Soc.* **1988**, *110*, 3622. (f) Tanko, J. M.; Drumright, R. E. *J. Am. Chem. Soc.* **1992**, *114*, 1844. (g) Mattiello, L.; Rampazzo, L. *J. Chem. Soc., Perkin Trans.* **1993**, 2243. (h) Liotier, E.; Mousset, G. Mousty, C. *Can J. Chem.* **1995**, *73*, 1488.

(3) (a) Elving, P. J.; Leone, J. T. *J. Am. Chem. Soc.* **1958**, *80*, 1021. (b) Wawzonek, S.; Gundersen, A. *J. Electrochem. Soc.* **1960**, *107*, 537.

(4) (a) Hermolin, J.; Kopilov, J.; Gileadi, E. *J. Electroanal. Chem.* **1976**, *71*, 245. (b) Kopilov, J.; Shatzmiller, S.; Kariv, E. *Electrochim. Acta* **1976**, *21*, 535. (c) Kopilov, J.; Kariv, E.; Miller, L. L. *J. Am. Chem. Soc.* **1977**, *99*, 3450.

(5) Lehninger, A. L. *Biochemistry*, 2nd ed.; Worth Publishers: New York, 1978; p 494.

(6) Monk, P. M. S. The Viologens: Physicochemical Properties, Synthesis and Applications of the Salts of 4,4′-Bipyridine; John Wiley and Sons: New York, 1998.

(7) (a) Leventis, N.; Chen, M.; Liapis, A. I.; Johnson, J. W.; Jain, A. *J. Electrochem. Soc.* **1998**, *145*, L55. (b) Leventis, N.; Gao, X. *J. Phys. Chem. B* **1999**, *103*, 5832.

(8) (a) Imahori, H.; Norieda, H.; Nishimura, Y.; Yamazaki, I.; Higuchi, K.; Kato, N.; Motohiro, T.; Yamada, H.; Tamaki, K.; Arimura, M.; Sakata, Y. *J. Phys. Chem. B* **2000**, *104*, 1253. (b) Fukushima, M.; Tatsumi, K.; Tanaka, S.; Nakamura, H. *Environ. Sci. Technol.* **1998**, *32*, 3948. (c) Moretto, L. M.; Ugo, P.; Zanata, M.; Guerriero, P.; Martin, C. R. *Anal. Chem.* **1998**, *70*, 2163. (d) Yuan, R.; Watanabe, S.; Kuwabata, S.; Yoneyama, H. *J. Org. Chem.* **1997**, *62*, 2494. (e) Nakamura, Y.; Kamon, N.; Hori, T. *Chem. Soc. Jpn.* **1989**, *62*, 551.

(9) Bookbinder, D. C.; Wrighton, M. S. *J. Electrochem. Soc.* **1983**, *130*, 1080.

(10) (a) Konishi, T.; Fujitsuka, M.; Ito, O.; Toba, Y.; Usui, Y. *J. Phys. Chem. A* **1999**, *103*, 9938. (b) Zahavy, E.; Seiler, M.; Marx-Tibbon, S.; Joselevich, E.; Willner, I.; Dürr, H.; O'Connor, D.; Harriman, A. *Angew. Chem., Int. Ed. Engl.* **1995**, *34*, 1005. (c) Inada, T. N.; Miyazawa, C. S.; Kikuchi, K.; Yamauchi, M.; Nagata, T.; Takahashi, Y.; Ikeda, H.; Miyahi, T. *J. Am. Chem. Soc.* **1999**, *121*, 7211. (d) Warren, J. T.; Chen, W.; Johnston, D. H.; Turro, C. *Inorg. Chem.* **1999**, *38*, 6187. (e) Borsarelli, C. D.; Braslavsky, S. E. *J. Phys. Chem. A* **1999**, *103*, 1719.

(11) (a) Leventis, N.; Sotiriou-Leventis, C.; Chen, M.; Jain, A. *J. Electrochem. Soc.* **1997**, *144*, L305. (b) Li, J.; Chen, G.; Dong, S. *Electroanalysis* **1997**, *9*, 834. (c) Tang, X.; Schneider, T. W.; Walker, J. W.; Buttry, D. A. *Langmuir* **1996**, *12*, 5921. (d) Tang, X.; Schneider, T.; Buttry, D. A. *Langmuir* **1994**, *10*, 2235. (e) Katz, E.; Itzhak, N.; Willner, I. *Langmuir* **1993**, *9*, 1392. (f) De Long, H. C.; Buttry, D. A. *Langmuir* **1992**, *8*, 2491. (g) Creager, S. E.; Collard, D. M.; Fox, M. A. *Langmuir* **1990**, *6*, 1617. (h) Lee, K. A. B. *Langmuir* **1990**, *6*, 709. (i) De Long, H. C.; Buttry, D. A. *Langmuir* **1990**, *6*, 1319.

(12) (a) Vögtle, F.; Plevoets, M.; Nieger, M.; Azzellini, G. C.; Credi, A.; De Cola, L.; De Marchis, V.; Venturi, M.; Balzani, V. *J. Am. Chem. Soc.* **1999**, *121*, 6290. (b) Jockusch, S.; Ramirez, J.; Sanghvi, K.; Nociti, R.; Turro, N. J.; Tomalia, D. A. *Macromolecules* **1999**, *32*, 4419. (c) Pollak, K. W.; Leon, J. W.; Fréchet, J. M. J.; Maskus, M.; Abruña, H. D. *Chem. Mater.* **1998**, *10*, 30.

(13) (a) Ruetten, S. A.; Thomas, J. K. *Langmuir* **2000**, *16*, 234. (b) Zhang, G.; Mao, Y.; Thomas, J. K. *J. Phys. Chem. B* **1997**, *101*, 7100. (c) Pfennig B. W.; Chen, P.; Meyer, T. J. *Inorg. Chem.* **1996**, *35*, 2898.

(14) (a) Vitale, M.; Castagnola, N. B.; Ortins, N. J.; Brooke, J. A.; Vaidyalingam, A.; Dutta, P. K. *J. Phys. Chem. B* **1999**, *103*, 2408. (b) Castagnola, N. B.; Dutta, P. K. *J. Phys. Chem. B* **1998**, *102*, 1696.

(15) (a) Bavykin, D. V.; Savinov, E. N.; Parmon, V. N. *Langmuir* **1999**, *15*, 4722. (b) Logunov, S.; Green, T.; Marguet, S.; El-Sayed, M. A. *J. Phys. Chem. A* **1998**, *102*, 5652. (c) Robins, D. S.; Dutta, P. K. *Langmuir* **1996**, *12*, 402.

(16) Jones, G., II.; Mabla, V. *J. Org. Chem.* **1985**, *50*, 5776.

(17) (a) Kosover, E. M.; Poziomek, E. J. *J. Am. Chem. Soc.* **1964**, *86*, 5515. (b) Grossi, L.; Minisci, F.; Pedulli, G. F. *J. Chem. Soc., Perkin II* **1977**, 943. (c) Grossi, L.; Minisci, F.; Pedulli, G. F. *J. Chem. Soc., Perkin II* **1977**, 948.

(18) Neta, P.; Patterson, L. K. *J. Phys. Chem.* **1974**, *78*, 2211.

(19) Frangopol, M.; Frangopol, P. T.; Trichilo, C. L.; Geiger, F. E.; Filipescu, N. *J. Org. Chem.* **1973**, *38*, 2355.

(20) Shu, C.-F.; Wrighton, M. S. *Inorg. Chem.* **1988**, *27*, 4326.

(21) Yoshiike, N.; Kondo, S.; Fukai, M. *J. Electrochem. Soc.* **1980**, *127*, 1496.

(22) Cupta, N.; Linschitz, H. *J. Am. Chem. Soc.* **1997**, *119*, 6384.

(23) (a) Leventis, N.; Gao, X. *J. Electroanal. Chem.* **2001**, *500*, 78. (b) Amatore, C.; Bonhomme, F.; Bruneel, J.-L.; Servant, L.; Thouin, L. *J. Electroanal. Chem.* **2000**, *484*, 1. (c) Rongfeng, Z.; Evans, D. H. *J. Electroanal. Chem.* **1995**, *385*, 201.

(24) Efange, S. M. N.; Michelson, R. H.; Remmel, R. P.; Boudreau, R. J.; Dutta, A. K.; Freshler, A. *J. Med. Chem.* **1990**, *33*, 3133.

(25) (a) Sonogashira, K.; Tohda, Y.; Hagihara, N. *Tetrahedron Lett.* **1975**, *50*, 4467. (b) Takahashi, S.; Kuroyama, Y.; Sonogashira, K.; Hagihara, N. *Synthesis* **1980**, 627.

(26) Back, K.; Huenig, S.; Reinold, P. *Tetrahedron* **1988**, *44*, 3295.

(27) (a) Streitweiser, A., Jr.; Reuben, D. M. E. *J. Am. Chem. Soc.* **1971**, *93*, 1794. (b) Patrick, T.; Disher, J. M.; Probst, W. J. *J. Org. Chem.* **1972**, *37*, 4467.

(28) Smith, M. B.; March, J. *March's Advanced Organic Chemistry. Reactions, Mechanisms, and Structure*, 5th ed.; John Wiley and Sons: New York, 2001, (a) p 330; (b) p 1217; (c) p 368; (d) p 98.

(29) Graham Solomons, T. W. *Solomons Organic Chemistry*; 6th ed.; John Wiley and Sons: New York, 1966; p 98.

(30) Munavalli, S.; Poziomek, E. J.; Landis, W. G. *Heterocycles* **1986**, *24*, 1883.

(31) (a) Cavallini, G.; Milla, E.; Grumelli, E.; Ravenna, F.; Grasso, I. *Farmaco, Ed. Sci.* **1958**, *12*, 853. (b) Breen, M. P.; Bojanowski, E. M.; Cipolle, R. J.; Dunn, W. J., III.; Frank, E.; Gearien, J. E. *J. Pharm. Sci.* **1973**, *62*, 847. (c) McCaustland, D. J.; Chien, P.-L.; Burton, W. H.; Cheng, C. C. *J. Med. Chem.* **1974**, *17*, 993. (d) Högberg, T.; Ulff, B.; Renyi, A. L.; Ross, S. B. *J. Med. Chem.* **1981**, *24*, 1499. (e) Bäckvall, J.-E.; Nordberg, R. E.; Nyström, J.-E.; Högberg, T.; Ulff, B. *J. Org. Chem.* **1981**, *46*, 3479. (f) Earley, J. V.; Gilman, N. W. *Synth. Commun.* **1985**, *15*, 1271. (g) Carvalho, I.; Miller, J. *Heterocycl. Commun.* **1995**, *1*, 403. (h) Takemoto, M.; Yamamoto, Y.; Achiwa, K. *Chem. Pharm. Bull.* **1996**, *44*, 853.

(32) (a) Wolffenstein, R.; Hartwich, F. *Chem. Ber.* **1915**, *48*, 2043. (b) Mirek, J. *Zesz. Nauk. Uniw. Jagiellon., Pr. Chem.* **1965**, *10*, 61. *Chem. Abstr.* **1967**, *66*, 37125h. (c) Carmellino, M. L.; Pagani, G.; Pregnolato, M.; Terreni, M. *Pestic. Sci.* **1995**, *45*, 227.

(33) (a) Crook, K. E.; McElvain, S. M. *J. Am. Chem. Soc.* **1930**, *52*, 4006. (b) Teague, P. C. *J. Am. Chem. Soc.* **1947**, *69*, 714.

(34) Mirviss, S. B. *J. Org. Chem.* **1989**, *54*, 1948.

(35) (a) Wawzonek, S.; Berkey, R.; Blaha, E. W.; Runner, M. E. *J. Electrochem. Soc.* **1956**, *103*, 456. (b) Given, P. H.; Peover, M. E. *J. Chem Soc.* **1960**, 385. (c) Umemoto, K. *Bull. Chem. Soc. Jpn.* **1967**, *40*, 1058. (d) Piljac, I.; Murray, R. W. *J. Electrochem. Soc.* **1971**, *118*, 1758. (e) Pekmez, K.; Can, M.; Yildiz, A. *Electrochim. Acta* **1993**, *38*, 607. (f) Revenga, J.; Rodriquez, F.; Tijero, J. *J. Electrochem. Soc.* **1994**, *141*, 330.

(36) (a) Paduszek-Kwiatek, B.; Kalinowski, M. K. *Electrochim. Acta* **1984**, *29*, 1439. (b) Kwiatek, B.; Kalinowski, M. K. *Aust. J. Chem.* **1988**, *41*, 1963.

(37) Bertie, J. E.; Lan, Z. *J. Phys. Chem. B* **1997**, *101*, 4111.

(38) The concave-down curvatures in Figure 3 are most probably due to the formation of HA-aggregates as the concentration of HA increases. An analysis of mechanisms I and II shows that the proton donor aggregation number should be also reflected into the slope of the $\Delta E_{1/2}$ vs log[HA] plots, which therefore should curve downwards with increasing [HA], as observed.

(39) (a) Bailey, T. D.; McGill, C. K. U.S. Patent 4,158,093, 1979. (b) Hart, L. S.; Killen, C. R. J.; Saunders: K. D. *J. Chem. Soc., Chem. Commun.* **1979**, 24. (c) Kutney, J. P.; Greenhouse, R. *Synth. Commun.* **1975**, 119.

(40) The reaction of **1** with base is most probably completed in the rotary evaporator (bath temperature ~50 °C) during solvent removal. Furthermore, it may be noted in Table 5 that with H_2O and *t*-BuOH as proton donors, no **8** was formed, whereas in the case of *t*-BuOH no **1** was recovered either. These results may seem contradictory because HO^- and RO^-, which are necessary for the formation of **9**, are byproducts of the formation of **8**, and therefore **8** should have been always present among the electrolysis products. We have noted, however, that even at slightly elevated temperatures (e.g., >30 °C) the reaction of **1** with either CH_3O^- or *t*-BuO^- is more complicated than a simple dequaternization, yielding along with **9** intractable products, which, according to the literature, should be attributed to pyridinium ring opening.[41] (In this regard, ^{1}H NMR spectra in CD_3CN show a consistent set of two doublets at 5.95 and 4.72 ppm with a coupling constant of 8.15 Hz, and more complicated patterns in the 2.4−4.6 ppm region.) The same NMR signals are detectable among the electrolysis products in the presence of CH_3OH and *t*-BuOH, and it is thus suggested that the yields of **8** and **9** are compromized by competing pyridinium ring opening side reactions.

(41) (a) Kavalek, J.; Lycka, A.; Machacek, V.; Sterba, V. *Collect. Czech. Chem. Commun.* **1975**, *40*, 1166. (b) Yakovlev, M. Yu.; Kadushkin, A. V.; Solov'eva, N. P.; Anisimova, O. S.; Granik, V. G. *Tetrahedron* **1998**, *54*, 5775.

(42) (a) Byker, H. J. *Proc. Electrochem. Soc.* **1994**, *94*, 2. (b) Byker, H. J. U.S. Patent 5,128,799, 1992. (c) Byker, H. J. U.S. Patent 4,902,108, 1990.